Investigation of Excited-State Proton Transfer in 2-Naphthol Derivatives Included in Langmuir−Blodgett Films

Agnieszka Mirończyk,[†] Andrzej Jankowski,*[,†] Antoni Chyla,[‡] Andrzej Ożyhar,[§] and Piotr Dobryszycki[§]

Institute of Biotechnology and Environmental Science, University of Zielona Góra, Monte Cassino 21b, 65-561 Zielona Góra, Poland, and Institutes of Physical and Theoretical Chemistry and of Organic Chemistry, Biochemistry and Biotechnology, Wrocław University of Technology, Wybrzeże Wyspiańskiego, 27 50-370 Wrocław, Poland

Received: July 3, 2003; In Final Form: April 21, 2004

The excited-state proton transfer in LB films of 2-naphthol-6-sulfonamide of dodecylamine (NSDA) has been studied by spectrofluorimetric methods. A modification of the composition of the atmosphere surrounding the samples enables an identification of emission peaks of the reactants, namely, an excited protonated (ROH*) form and a dissociated (RO^-*) form taking part in the excited-state deprotonation (ESDP). The mechanism of proton transfer and the nature of the proton acceptor were assessed from the study of separated emission spectra, taken at various experimental conditions and for various film layouts. The estimated rate of proton transfer was between 5×10^8 and 5×10^9 s^{-1}. The results concerning ESDP in LB films suggest that water molecules, probably forming chains of hydrogen bonds ("proton wires"), and carboxyl groups forming a type of hydrogen bonds with a proton donor could be the main proton acceptors.

1. Introduction

Proton transfer in ordered molecular assemblies such as Langmuir−Blodgett (LB) films can be considered as a good model for proton movement in biological membranes, in energy transformation systems (photosynthesis,[1] respiration), and in enzymes.[2] It is known that vectorial proton translocation in these systems plays a crucial role in their proper function.[3,4] Because LB films have often been proposed as experimental systems for modeling cell membranes, it would be interesting to study the effect of unidirectional proton movement across a thin LB film. The problem of excited-state proton transfer in LB films has been investigated by Il'ichev et al.[5] and by Zaitsev.[6] In ref 5, intramolecular proton transfer between phenolic and carbonyl groups in acyl-substituted 1-naphthol was described, but no intermolecular excited-state reaction was observed for alkyl derivatives of 1- or 2-naphthol. To study the title problem, we have chosen the 2-naphthol-6-sulfonamide derivative of dodecylamine (NSDA) as a fluorescent compound showing excited-state deprotonation (ESDP) that is suitable for inclusion into an LB film. This compound contains an electron-withdrawing substituent ($-SO_2NH-$) that is expected to enhance proton transfer

1.1. Excited-State Processes in LB Films. In the case of 2-naphthol derivatives in solution, ESDP is usually manifested by dual fluorescence where two emission peaks represent the originally excited (ROH*) and ionic (RO^-*) forms of the fluorophore[7] (see Scheme 1). Fluorescence spectra with two bands can be observed for 2-naphthol derivatives in LB films.

SCHEME 1: Excited-State Processes in 2-Naphthol Derivatives in a Hydrophobic Medium[a]

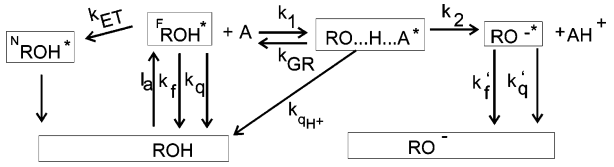

[a] ROH* is the originally excited neutral, and RO^-* ionic form of NSDA. I_a Is the rate of excitation. k_f and k_q are the rate constants for the fluorescence and radiationless deactivation of ROH*, respectively. k_f' and k_q' are the rate constants for the fluorescence and radiationless deactivation of RO^-*, respectively. k_{ET} is the rate constant for energy transfer between the F and N domains. k_1 and k_2 are the rate constants for proton transfer along a hydrogen bond and for charge separation, respectively. The product k_1k_2 is treated as an overall deprotonation rate constant and designated as k_{DP}. k_{GR} is the rate constant for geminal recombination of a proton with an excited chromophore. k_{qH^+} is the rate constant for quenching by aromatic ring protonation.

However, assignment of these bands to two fluorophore forms participating in ESDP is not unequivocal as in the case of solutions. If in aqueous solutions or organic solvents, the role of proton acceptor (A) can be played by either the cluster of water molecules ($[H_2O]_n$, $n > 4$) or other polar molecules;[8] in LB films, which are composed predominantly of hydrophobic chains of amphiphilic molecules, no considerable concentration of polar and charged species such as $[H_2O]_n$, H^+, H_3O^+, OH^-, or NH_4^+ can be expected. Therefore, the question arises as to what is the proton acceptor in LB films and how can unfavorable interactions between the positive charge of the proton and a hydrophobic medium be avoided.

Moreover, it is known that a condition for ESDP to be observed by steady-state fluorescence is a favorable relation of its rate to the rates of other excited-state processes involving the fluorophore.[7] In solutions, the escape of the proton or the proton acceptor complex (AH^+) is usually fast enough to

* Corresponding author: A. Jankowski E-mail: JJJ@WCHUWR.CHEM.UNI.WROC.PL.
[†] University of Zielona Góra.
[‡] Institute of Physical and Theoretical Chemistry, Wrocław University of Technology.
[§] Institute of Organic Chemistry, Biochemistry and Biotechnology, Wrocław University of Technology.

10.1021/jp035919u CCC: $27.50
Published on Web 05/26/2004

compete successfully with the decay of the excited state of the fluorophore. In LB films, the process of charge separation by means of diffusion might be too slow to enable observation of fluorescence from the deprotonated fluorophore.[8,9] The possibility of observing ESDP by steady-state fluorescence depends on the ratio of its rate to the rates of other excited-state processes.

The excited-state processes in our samples can be represented in Scheme 1.[7,10]

Model studies of fluorescent dyes in LB films[11] suggest that the fluorophore molecules aggregate in the film, forming fluorescent (F) and nonfluorescent (N) domains. The aggregation leads to a considerable reduction of the fluorescence quantum yield and a red shift of the band that can be understood as exciton effects.[12] Radiationless energy transfer (ET) from F to N also gives a reduction of the lifetime of the excited state of the fluorophore.

The rate constants k_{GR} and k_{qH+} depend on H^+ migration through a hydrophobic medium and, therefore, can be expected to be lower than k_1 and k_{ET}. The value of k_2 is discussed in section 4. We assume initially that the processes corresponding to k_{GR} and k_{qH+} involving the complex $[RO^-\cdots H\cdots A^+{}^*]$ do not significantly influence the steady-state fluorescence of NSDA in LB films even if such a complex in this medium really exists. This assumption is to be verified by further results.

1.2. Calculation of the Rate Constant of ESDP (k_{DP}). If the rate constants k_{GR} and k_{qH+} are neglected, the rate constants of all processes involving the complex $[RO^-\cdots H\cdots A^+{}^*]$ can be replaced by the deprotonation rate constant k_{DP}. In this way, one can obtain expressions 1a and 1b for the time-dependent concentrations of the ESDP reactants.

$$d[RO^-{}^*]/dt = k_{DP}[ROH^*] - (k'_f + k'_q)[RO^-{}^*] \quad (1a)$$

$$d[ROH^*]/dt = I_a - (k_f + k_q + k_{DP} + k_{ET})[ROH^*] \quad (1b)$$

Within the steady-state approximation ($d[ROH^*]/dt = d[RO^-{}^*]/dt = 0$), one can derive expressions for the fluorescence quantum yields of the ionic form, $RO^-{}^*$ (Φ'), and of the ROH* form (Φ) and subsequently calculate the ratio of the relative fluorescence quantum yields (see the Appendix) as

$$(\Phi'/\Phi)(\Phi_0/\Phi'_0) = k_{DP}\tau_0 \quad (2)$$

where Φ_0 and Φ'_0 are the fluorescence quantum yields of ROH* and $RO^-{}^*$, respectively, in absence of ESDP, whereas Φ and Φ' are the corresponding fluorescence quantum yields in the presence of ESDP. τ_0 represents the excited-state lifetime of ROH*. The ratio (Φ_0/Φ'_0) can be treated as a constant, characteristic for a given pair of reactants.

Equation 2 is identical to the equation derived by Weller[7a] for excited acids in solution in absence of a proton donor (H_3O^+).

It follows from eq 2 that the ratio Φ'/Φ appears to be proportional to k_{DP}. Therefore, the determination of the ratio Φ'/Φ, or a measurement of the ratio of the fluorescence intensities of the $RO^-{}^*$ and ROH* forms (E_{M2}/E_{M1}), makes possible an estimation of the rate of ESDP. This might help to understand the mechanism of proton transfer in ordered hydrophobic media such as biological energy transformation systems.

2. Materials and Methods

Synthesis. The 2-naphthol-6-sulfonamide derivative of dodecylamine (NSDA; see Figure 1) was synthesized as described in ref 13.

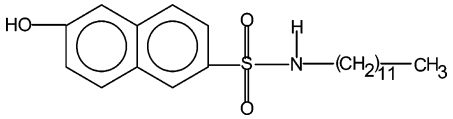

Figure 1. Structure of NSDA.

SCHEME 2: Types of Film Layouts in Our Samples[a]

(1) o--- o--- T : N+X (4) o--- ---o N+X : N+X

(2) o--- o--- ---o T : N+X : N+X (5) ---o o--- N+X : N+X

(3) o--- ---o o--- T : N+X : N+X (6) o--- o--- ---o N+X : N+X : N+X

[a] Abbreviations: N, NSDA; T, tricosanoic or stearic acid; X, stearic acid (S), octadecylamine (O), or null (in samples of pure NSDA); ○, hydrophilic head; - - -, hydrophobic tail.

2.1. Formation of Langmuir−Blodgett (LB) Films. NSDA solutions in chloroform were used for the deposition of LB layers. The films were deposited onto quartz plates by means of a KSV−5000 (KSV Instruments Ltd., Espoo, Finland) trough. In some samples, pure NSDA solutions in $CHCl_3$ were used, and in others, mixtures with stearic acid or octadecylamine containing NSDA (0.05−0.2 mol fraction) were used.

LB films containing NSDA were deposited onto quartz plates by means of a vertical dipping procedure. LB films of pure NSDA and binary systems of NSDA with stearic acid or octadecylamine (0.05−0.2 mol fraction) were used. The surface tension, transfer ratio, barrier speed, and plunging and lifting speeds were controlled during the deposition. The average area per molecule estimated for pure NSDA film was 32.3 Å^2. Typical transfer isotherms for all materials deposited are given in Figures S1−S4 of the Supporting Information.

To improve the anchoring of NSDA, prior to its deposition, substrates were covered with a monomolecular layer of stearic or tricosanoic acid with hydrophilic groups directed toward the quartz plate. Further procedures in the LB film deposition depend on the type of layout required. The head-to-tail (○- - -○- - -) layout was obtained during upstroke movements of the substrate, initially placed under water. Before consecutive dippings, the films were left to dry, and the water surface was cleaned. A repetition of this procedure gives the required layout. In most cases, the transfer ratio was close to 1.

To investigate the influence of the film organization on the rate of ESDP and the reaction conditions, we prepared samples of various molecular arrangements within the film. Different types of film layouts are presented in Scheme 2. No dependence of the transfer ratio and other parameters of the deposition procedure on the type of film layout was noticed.

2.2. Spectrophotometric and Spectrofluorimetric Measurements. The absorption spectra were taken by means of a UV-2102 P (Shimadzu Corporation, Kyoto, Japan) instrument. Spectrofluorimetric steady-state measurements were performed on an SF1 module apparatus (OPTEL Ltd., Opole, Poland). The samples were excited with light beams of wavelength 315−320 nm and analyzed at 340−600 nm. Some fluorescence and phosphorescence spectra were taken by Fluorolog-3 Spex instrument [excitation at 313 nm, analysis at 340−700 nm using a cutoff filter (Schott) for λ < 320 nm].

In the spectrofluorimetric measurements, the angle between the incident exciting beam and the plate surface was set to about 60°, and precise adjustment was performed manually by reducing to a minimum the scattered light of λ near to $\lambda_{excit.}$ Even so, in some experiments, the reflected and scattered light (630−640 nm) disturbed the measurements in the high-wavelength spectral range (550−600 nm).

The composition of the atmosphere surrounding the sample during the measurements was modified by the addition of 0.05 cm^3 of various solvents (e.g., glacial acetic acid, NH_3, or H_2O) on the bottom of the closed cuvette.

The fluorescence lifetimes of ROH* form were measured on an Aminco 48000 phase and modulation instrument using the software provided by the manufacturer. In these measurements, the sample was excited with monochromatic light (313 nm), and the emission at $\lambda > 320$ (Schott WG 320 cutoff filter) was analyzed.

The fluorescence spectra were corrected with respect to the detector response as described by Lakowicz,[14] and the fluorescence quantum yields were calculated from the following equation 3[14,15]

$$\Phi_x = (F_x A_{st}/F_{st} A_x)\Phi_{st} \tag{3}$$

where F_x is the corrected fluorescence intensity at the band maximum, A_x is the absorbance at the exciting wavelength of the sample, and F_{st} and A_{st} are the analogous values for the standard. As a standard, the 2-naphthol-6-sulfonamide derivative of glycine in methanol solution ($\Phi_{st} = 0.18$[16]) was used. The refractive indexes of the films were not measured and were assumed to be near to 1.0

2.3. Resolution of the Fluorescence Spectra into Component Bands. By analogy to 2-naphthol derivatives in solutions, the presence of two fluorescence peaks of the ROH* and RO^-* forms of NSDA could be expected. On the other hand, band broadening and a spectral shift can sometimes cause a merging of these bands into one broad peak. For a successful separation of the fluorescence spectra of NSDA in LB films, it was necessary to know the shapes and positions of the ROH* and RO^-* contributions.

The fluorescence spectra of NSDA in an LB film placed in an atmosphere of acetic acid vapor were used as a standard for the ROH* component in the emission spectrum. Similarly, spectra taken in an atmosphere saturated with NH_3 were used as a standard for the RO^-* component band. (The reason for using these spectra as standards for the ROH* and RO^-* components is the analogy of the band shapes and positions of these spectra with the component spectra of NSDA and its analogues in organic solvents. This problem is explained in more detail below.) Using these standards, one can provisionally separate the fluorescence spectra of NSDA in LB films.

Parameters describing the shape of the component bands derived from this procedure were applied to a log-normal function{4}.[17]

$$F_\lambda = [E_M b/(\lambda - a)] \exp(c^2) \exp\{-1/(2c^2)[\ln(\lambda - a)/b]^2\} \tag{4}$$

where F_λ is the fluorescence intensity at a given wavelength; E_M is the maximum fluorescence intensity of a given band; and the parameters c, b, and a have the following meanings

$$c = \ln(RO)/(2 \ln 2)^{0.5}$$

$$b = H[RO/(RO^2 - 1)] \exp c^2$$

$$a = L_M - H[RO/(RO^2 - 1)]$$

Other parameters are explained in Figure 2.

It was possible to change six parameters (E_M, H, and L_M or E_M, H, and RO for each of the two bands) in our software, so that the best fit to our experimental data was obtained as a sum

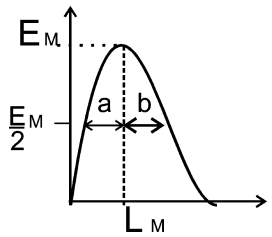

Figure 2. Explanation of the meanings of the parameters of the log-normal function (eq 4). $RO = B/A$, $H = a + b$.

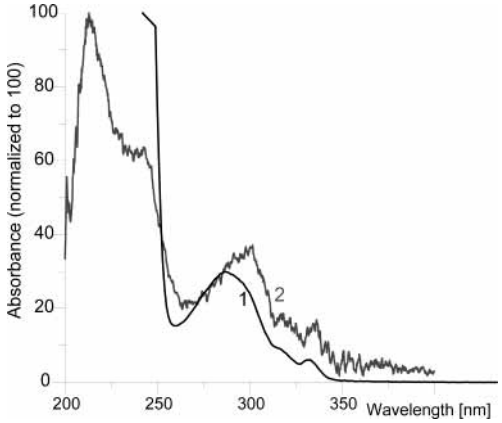

Figure 3. Absorption spectra of NSDA (1) in hexane and (2) in an LB film (three layers thick).

of two log-normal functions (the functions given by eq 4). One of these functions corresponds to the ROH* component band characterized by band height E_{M1} and band maximum position L_{M1}, and the other corresponds to the RO^-* component with band height E_{M2} and band maximum position L_{M2}. The ratio of the heights of these two bands obtained by the separation procedure, E_{M2}/E_{M1}, is a measure of the relation between the fluorescence intensities of the two fluorophore forms. This value can be also treated as some measure of the rate of ESDP.

3. Results

3.1. Spectral Characteristics of Three Layers of NSDA in LB Films. As presented in Figure 3, the absorption spectrum of a three-layer-thick LB film of NSDA (curve 2) resembles the spectrum of a solution of the same substance in hexane (curve 1). The positions of two lowest-energy bands are only slightly red-shifted with respect to the positions of equivalent bands in hexane. The shift of the higher-energy band is more pronounced.

The fluorescence quantum yield is greatly reduced: for 2-naphthol derivatives in methanol solution, the value of $\Phi = 0.18$ has been reported,[16] and for three layers of NSDA in an LB film, we obtained the value 0.005 (see also Tables 1 and 3). This picture, consisting of a red shift and a decrease of Φ, is typical for organic fluorophores incorporated into LB films, and on the basis of this analogy, the effects observed must be attributed to collective excitation (exciton effects) and energy transfer from fluorescent (F) to nonfluorescent (N) centers.[11]

3.2. Separated Fluorescence Bands of the RO^-* and ROH* Forms. The fluorescence spectra of the sample of a three-monolayer-thick LB film of NSDA are shown in Figure 4 (cf Figures S5−S10 of the Supporting Information).

For the purpose of separating the fluorescence bands, we compared the spectra taken in neutral atmosphere with those recorded in acetic acid or ammonia vapor (see Experimental

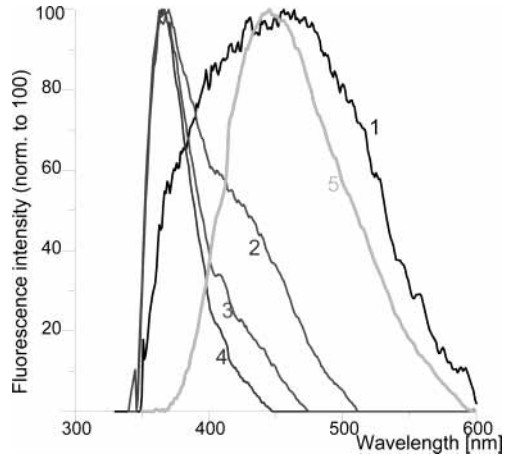

Figure 4. Fluorescence spectra of three layers of NSDA (1) in neutral atmosphere, (2) in CH_3COOH for 1 min, (3) in CH_3COOH for 5 min, (4) in CH_3COOH for 10 min, and (5) in NH_3 for 5 min.

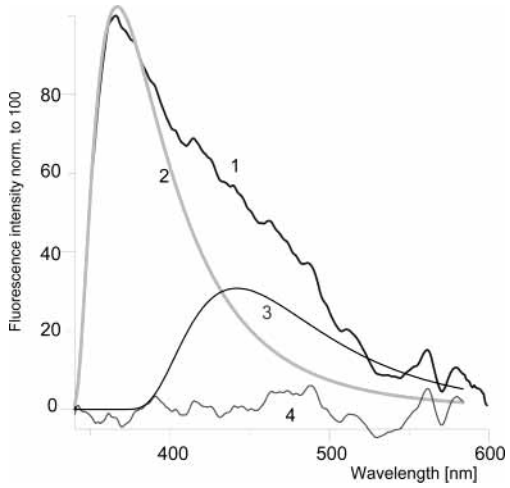

Figure 5. Separation of the fluorescence spectrum of sample TNONO.3 (film layout, ○- - - ○- - - - - -○; T:(N + O):(N + O)) into component ROH* and RO^-* bands: (1) experimental spectrum in neutral atmosphere, (2) ROH* component, (3) RO^-* component, (4) error distribution. Fit parameters: $c^2 = 3.02$, $E_{M1} = 105$, $E_{M2} = 29$, $H_1 = 53$, $H_2 = 71$, $L_{M1} = 375$ (367), $L_{M2} = 460$ (442) nm, $RO_1 = 1.908$, $RO_2 = 1.447$. The meanings of the abbreviations E_{M1}, E_{M2}, L_{M1}, L_{M2}, RO_1, and RO_2 are the same as in Scheme 2 and Figure 2.

Section). It can easily be noticed (see, e.g., curve 1 of Figure 4 and curve 1 of Figure 5) that the two bands, constituents of the dual fluorescence, assigned to the ROH* and RO^-* species can be distinguished in the fluorescence spectra of LB films of NSDA. One can believe that the emission band in acetic acid represents the pure ROH* band because the shape of the band and its position (360 nm) are very much like those of NSDA in methanol solution (363 nm), for which a single ROH* band is observed. Moreover, during incubation in acetic acid vapor, the emission band at 450 nm gradually disappears (Figure 4), and the band at 360 nm subsequently increases; the opposite effect is visible in ammonia.

Similarly, the spectrum in ammonia vapor (Figure 4, curve 5) resembles that of the RO^-* species observed in solution. NH_3 ($pK_a = 9.2$), in principle, can abstract the proton from the phenol group ($pK_a = 10$). However, the absorption spectra of our samples in ammonia vapor (results not shown) are identical to the spectrum presented in Figure 3 (curve 2) that was obtained in neutral atmosphere. If the ionic form (RO^-*) was present, a red shift of the absorption spectrum, analogous to that observed in solution, would be found. It must be concluded that, in ammonia, NSDA molecules occur in the ground state only in the protonated form. Spectrum 5 in Figure 4 must not be treated as an effect of a direct excitation of the RO^- form. The spectral shift visible must be attributed to a great enhancement of the rate of ESDP in NSDA molecules due to the presence of NH_3 as a proton acceptor.

These changes of fluorescence, justify the use of the spectra in acetic acid and ammonia vapor as standards for band separation, as was described in the Experimental Section. For more details concerning the interactions of components of LB films with the outer environment, see refs 11d and 11e.

The results of the separation of the fluorescence spectrum of NSDA (N), mixed with octadecylamine (O) included in an LB film into component bands for ROH* and RO^-* are shown in Figure 5.

The same procedure applied to the fluorescence spectra of other samples has shown that all parameters determining the band shape of the protonated form (RO_1, E_{M1}/H_1), precisely determined by our procedure, are similar in the standard and in the separated spectra. The characteristics of the RO^-* band are less consistent, which is probably due to various contributions from the reflected and scattered light (640 nm). It must be noticed, however, that our samples seem to be optically clear and transparent.

3.3. Ratio of the Fluorescence Intensities of the RO^-*/ ROH* Forms (E_{M2}/E_{M1}) for Various Film Layouts. The fluorescence intensities of the bands of RO^-* and ROH* in various film layouts were studied to recognize the influence of film layout on the rate of ESDP. It was assumed, therefore, that the ratio of the intensities of these bands (E_{M2}/E_{M1}) is proportional to the rate of ESDP. The results are presented in Table 1.

The film layout containing only one layer of NSDA diluted with stearic acid [the type of layout labeled TNS (no. 6) in Table 1] is characterized by a markedly higher E_{M2}/E_{M1} value, and thus a higher rate of ESDP, than other types of samples. Generally, the films of the fluorophore diluted with stearic acid (nos. 6−9) in most cases reveal higher E_{M2}/E_{M1} ratios than analogous undiluted films (nos. 1−5). This suggests that accessibility to the outer atmosphere and the presence of stearic acid enhance ESDP.

The dilution of the fluorophore with octadecylamine [the type of layout labeled TNONO (no. 8) in Table 1] influences the spectrum and the value of E_{M2}/E_{M1} essentially in the same way, although the observed wavelength, L_{M1}, is slightly blue-shifted.

The layouts of layers in which NSDA molecules are near the outer surface of the film, irrespective of dilution, show higher rates of ESDP than those with the fluorophore layer in inner positions. Moreover, the samples with head-to-head dispositions of the fluorophores (Table 1, nos. 3, 5, and 9) have higher contributions of the E_{M2} form in the fluorescence than the others.

3.4. Estimation of the Rate of ESDP. In all investigated samples, an emission from the ionic (RO^-*) form can be observed. This leads to the conclusion that the rate constant of ESDP (k_{DP}) must be at least comparable to that of fluorescence ($k_f = 1/\tau_0$, where τ_0 is the lifetime of the excited state of NSDA in the absence of ESDP).

Bearing in mind Scheme 1, one can now rewrite eq 2 in the following form (5) where the symbols used have the same meaning as in eq 2

$$k_{DP} = (1/\tau_0)(\Phi'/\Phi)(\Phi_0/\Phi_0') \qquad (5)$$

Assuming that the ratio of the fluorescence quantum yields of the ROH* and RO^-* forms in absence of ESDP (Φ_0/Φ_0') is

TABLE 1: Mean Values of the Ratio of the Fluorescence Intensity of RO$^-$* to that of ROH* (E_{M2}/E_{M1}), Fluorescence Quantum Yield (Φ), and Position of the ROH* Band Maximum (L_{M1}) for Various Layouts

no.	film layout	label[a]	E_{M2}/E_{M1}[b]	Φ	L_{M1}[b] (nm)
1	O- - - O- - - T:N	TN	0.69	3.0×10^{-3}	378
2	O- - - O- - - - - -OT:N:N	TNN	0.19	2.2×10^{-3}	384
3	O- - - - - -O O- - - T:N::N	TNN	0.47	3.0×10^{-3}	380
4	O- - - - - -ON:N	NN	0.31	5.3×10^{-3}	385
5	O- - - - - -O O- - - N:N:N	NNN	0.86	1.2×10^{-4}	378
6	O- - - O- - - T:(N + S)	TNS	2.03	1.0×10^{-2}	369
7	O- - - O- - - - - -OT:(N + S):(N + S)	TNSNS	0.69	3.0×10^{-3}	378
8	O- - - O- - - - - -OT:(N + O):(N + O)	TNONO	0.42	5.0×10^{-3}	368
9	O- - - - - -O O- - - T:(N + S):(N + S)	TNSNS	0.67	4.7×10^{-3}	385

[a] Abbreviations: T, tricosanoic acid; N, NSDA; S, stearic acid; O, octadecylamine. [b] Values yielded by the band separation procedure. Each value is a mean from 3−10 independent measurements.

TABLE 2: Values of the ESDP Rate Constant (k_{DP}) and the Sum of k_{DP} Plus the Rate Constant for Energy Transfer from F to N centers (k_{ET}) for NSDA in LB Films

no.	sample	E_{M2}/E_{M1}	k_{DP} (s^{-1})[a]	$k_{DP} + k_{ET}$ (s^{-1})[b]
1	TN.a	0.715	3.5×10^8	4.6×10^9
2	TNS.1	1.340	6.7×10^8	1.6×10^9
3	TNSNS.z	0.473	2.3×10^8	3.7×10^8
4	TNSNS.5	0.575	2.9×10^8	7.7×10^8
5	NNN.1	0.100	5.0×10^7	6.0×10^8

[a] Equation 5. [b] Equation 6.

the same as that determined for 2-naphthol derivatives in methanol solution[16] ($\Phi_0/\Phi_0' = 0.5$) and that the excited-state lifetime in the absence of ESDP (τ_0) in samples diluted with stearic acid is $\tau_0 = 1$ ns[16] allows an estimation of the values of k_{DP} for our samples (Table 2).

For LB films containing undiluted NSDA, a similar value of τ_0 was used because it was the highest value of τ measured for such samples (Table 3).

The mean lifetime of the excited state of ROH* in the presence of both deprotonation and energy transfer can be written as

$$\tau = 1/(k_f + k_q + k_{DP} + k_{ET}) \quad (6)$$

and in the absence of these last two processes as

$$\tau_{00} = 1/(k_f + k_q) \quad (7)$$

Taking into account these expressions for τ_{00} and τ, as well as the lifetime values of Table 3, it is possible to calculate the sum of rate constants ($k_{DP} + k_{ET}$) from eq 8. The estimated data for ($k_{DP} + k_{ET}$) are given in Table 2.

$$(k_{DP} + k_{ET}) = 1/\tau - 1/\tau_{00} \quad (8)$$

For NSDA diluted with stearic acid, for τ_{00}, we inserted into eq 8 the lifetime value τ_{AA} determined for the sample in acetic acid vapor. For undiluted samples, the value $\tau_{00} = 1.03$ ns (Table 2, no. 5) was applied. As the mean lifetimes of the excited state of NSDA molecules in LB film in the presence of ESDP and ET (τ), we used the centers of the lifetime distributions functions determined by our instrument. A comparison of Tables 1 and 2 shows that the fluorescence quantum yield of NSDA greatly increases in acetic acid as compared to that in neutral solution; the enhancement of Φ in ammonia is less conspicuous.

The values of k_{DP} in Table 2 fall within the same range (10^7−10^9 s^{-1}) as $1/\tau_{00}$ for 2-naphthol analogues in solution,[13,16] whereas the values of k_{ET}, calculated from the results of Table 2 as the difference ($k_{DP} + k_{ET}$) − k_{DP}, in most cases, are higher than k_{DP}.

3.5. Influence of Water on the Fluorescence Spectra of NSDA in LB Films. As stated in section 3.3, the films in which the NSDA layer is in an external position, exposed to contact with outer atmosphere, exhibit the highest contribution of RO$^-$* fluorescence. Likewise, for ESDP, in mixtures of organic solvents with water,[7,8,16] one can now assume that the role of proton acceptors in LB films is played by the water molecules adsorbed in the film.

The samples in which NSDA was not diluted by aliphatic acid or amine show a very pronounced impact of water on the fluorescence spectra (Figure 6), in contrast to the undiluted samples (results not shown).

In the dried sample, the higher-energy band due to the ROH* form is centered at wavelength 383 nm (the results of band

TABLE 3: Lifetimes and the Fluorescence Quantum Yields of NSDA in LB Films (ROH* Form) in Neutral Atmosphere (τ_n, Φ_n), in Acetic Acid (τ_{AA}, Φ_{AA}), and in Ammonia (τ_{NH_3}, Φ_{NH_3})

no.	sample[a]	τ_n (ns)	Φ_n	τ_{AA} (ns)	Φ_{AA}	τ_{NH_3} (ns)	Φ_{NH_3}
1	TN.a	0.16 D[b]	1.9×10^{-3}	0.59 M[c]	7.7×10^{-3}	0.42 M	3.4×10^{-3}
2	TNS.1	0.27 D	7.4×10^{-3}	0.46 M	1.7×10^{-2}	−	
3	TNSNS.z	0.62 D	1.1×10^{-2}	0.81 M	3.0×10^{-2}	−	
4	TNSNS.5	0.44 D	2.0×10^{-3}	0.66 D	−	−	
5	NNN.1	0.64 D	1.7×10^{-4}	1.03 D	3.7×10^{-4}	0.64 D	1.8×10^{-4}

[a] Sample nos. 1−4 are the same as in Table 2. Sample 5 has the film layout: O- - - O- - - - - -O N:N:N. [b] Lifetime distribution (Gaussian). Width of the Gaussian distribution function at half-maximum = 0.5−1 ns. For some samples (i.e., nos. 1, 2, and 4), the half bandwidth was higher than the maximum value itself. [c] Single-exponential decay.

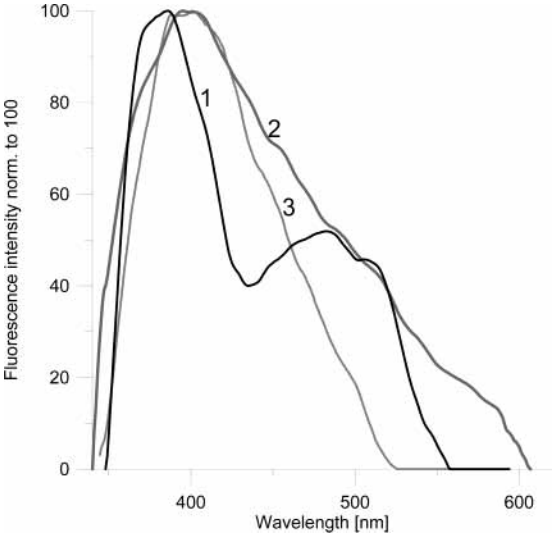

Figure 6. Influence of the water content in the atmosphere on the fluorescence spectrum of the sample TN.a (layout ○- - - ○- - -; T:N) corrected and normalized to 100 fluorescence spectra of sample TN.a: (1) immediately after drying in a desiccator over SiO_2, (2) 1 min after addition of 0.05 cm^3 of H_2O to the closed cuvette, (3) 10 min after water addition.

separation are not shown), whereas in air-equilibrated conditions, this band is positioned at 370 nm (Table 1, no. 1). The maximum of the lower-energy band (of the RO^-* form) in the dry sample is positioned at 496 nm, whereas in the air-equilibrated sample, this band is at 430 nm. Both bands are much better resolved in the dried sample. Band asymmetry (RO_1, RO_2) and other parameters determined by the oscillatory structure such as E_{M1}/H_1 and E_{M2}/H_2 are also different for the dried and air-equilibrated samples.

The ratio of E_{M2}/E_{M1} obtained from the band separation procedure for dried sample TN.a (Table 2, no. 1) equals 0.366, whereas for the same sample equilibrated in air, the value of 0.72 was found. This indicates that increasing the water content considerably enhances the rate of ESDP but the decrease resulting from drying is not more than 50%.

If water were the only proton acceptor in the LB films, no contribution from the deprotonated species, immediately after drying, would be expected. It follows that bulk clusters of water molecules are probably not the unique proton acceptors in LB films. On the other hand, absorbed water molecules can migrate into the film, and we cannot exclude the likelihood that, even after drying, a few water molecules remain in the sample, most probably forming small assemblies (linear clusters).

4. Discussion and Conclusions

Even if water assemblies were a main proton acceptor for excited NSDA in LB films, charge separation by the diffusion of H_3O^+ seems very unlikely as a mechanism. Literature data concerning some biological systems[1b] indicate that even small numbers of water molecules can form chain structures of hydrogen-bonded units, particularly if they meet together in a hydrophobic medium, as confirmed by X-ray structures of proteins in a hydrated crystalline state.[1b,18,19] An unfavorable interaction of a positive charge with a hydrophobic medium can be decreased if the proton in state II (Figure 7) is in a more polar environment than that in state I.

Because of this effect, the value of k_2 in Scheme 1 for fluorophores encountering a suitable proton acceptor in their vicinity can be higher than the rate constants for most other excited-state processes.

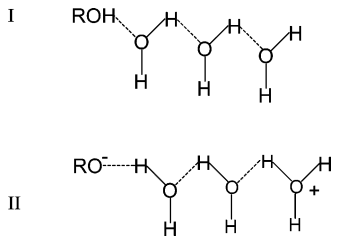

Figure 7. Probable mechanism of proton transfer in a hydrophobic medium such as an LB film.

From the values of ($k_{DP} + k_{ET}$) (Table 2), it can be concluded that ESDP and energy transfer from F to N centers (ET) dominate over remaining excited-state processes in NSDA (Scheme 1). This would justify neglecting other processes involving the hydrogen-bonded complex [RO···H···A*] in our derivation of eq 2.

Moreover, the fact that the samples in which NSDA was mixed with stearic acid (S) show higher values of E_{M2}/E_{M1} than undiluted samples (Table 1) suggests that the carboxyl group of S can also play a role of primary proton acceptor for the excited NSDA. Simple thermodynamic considerations indicate that the probability of proton transfer to a carboxyl group is low. On the other hand, theoretical calculations by Sokalski et al.[21] and Ushiyama et al.[22] show that double proton transfer in a system such as

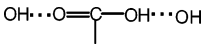

under conditions of conformational strain (see also ref 18) might be responsible for proton translocation. Other structures forming chains of hydrogen bonds (e.g., OH···OH, OH ···SO_2−NH) might be present in the aggregates of NSDA in LB films.

Opposite to the influence of long-chain fatty acids is the effect of acetic acid. It consists of the inhibition of ESDP by instantaneous reprotonation of RO^-*. A low molecular volume of acetic acid admits conformational freedom of double hydrogen-bond formation, which allows, in contrast to fatty acids, for the creation of a stable complex between acetic acid and NSDA in the ground state.[16]

The influence of ammonia on the fluorescence of NSDA in LB films is analogous to that of acetic acid, but NH_3 promotes ESDP. Because acetic acid inhibits ESDP, the difference between the inverse excited-state lifetimes ($1/\tau_{NH_3} - 1/\tau_{AA}$) can be recognized as the rate constant of ESDP in NH_3. For the sample TN.a (Table 3, no. 1), one obtains $k_{DP} = 1/\tau_{NH_3} - 1/\tau_{AA} = 6.8 \times 10^8\ s^{-1}$.

The low fluorescence signals from LB films and uncertainty of lifetime estimation decrease the precision of Φ and k_{DP} determinations. Because of the lack of precise lifetime values, we used only centers of lifetime distributions instead. (This procedure is common for dyes in LB films.[11a]) It should be stressed here that the values of k_{DP} and k_{ET} obtained by our methods are consistent with the basic relations of the excited-state processes in our fluorophore.

A general conclusion that can be drawn from our results is that the ESDP process can be observed in NSDA in LB films and its rate constant is in the range of 10^8−$10^9\ s^{-1}$.

This finding differs from the results of Il'ichev et al.[5] who found that alkyl-substituted naphthols do not show ESDP in LB films. Especially interesting is a comparison to the alkyl derivatives of 1-naphthol, for which no ESDP has been observed,[5] even though its acidity in the excited state in water solution ($pK_a^* = 0.4$) is near that of our 2-naphthol-6-sulfonamide derivatives having pK_a^* values in the range of

0.32−0.70.[13] It has been suggested[7c,d] that ESDP in 1-naphthol has a different mechanism that that of 2-naphthol, for which it consists of solvent-dependent vibronic coupling of the two lowest-lying excited states (L_a and L_b). In LB films, no solvent effect on L_a-L_b state mixing is possible, but an interaction of electronic transitions in the fluorescent (F) aggregates[12] probably could also induce a similar effect. In contrast, in 1-naphthol and its derivatives, intramolecular energy redistribution is responsible for ESDP.[8b] This process appears to be inhibited in the solid state (LB films), which might result in the above-mentioned difference in the behaviors of 1- and 2-naphthol derivatives.

A mechanism of proton transfer similar to that operating in LB films is probably responsible for "proton leakage" in biological membranes outside the proton channels, which counteracts the formation of a proper proton gradient and thus inhibits the production of ATP.[3]

Supporting Information Available: Figures S1−S11 comprising transfer isotherms of all substances deposited; fluorescence spectra of undiluted NSDA, recorded in neutral atmosphere and in acetic acid and ammonia vapor; fluorescence spectra of NSDA mixed with stearic acid or with octadecylamine; and fluorescence spectra of diluted NSDA, recorded in acetic acid and ammonia vapor.

Appendix

From the steady-state approximation, we have

$$[RO^-{}^*] = (k_{DP}[ROH^*])/(k_f' + k_q') \qquad (A1)$$

and

$$[ROH^*] = I_a/(k_f + k_q + k_{DP} + k_{ET}) \qquad (A2)$$

Using an expression for the fluorescence quantum yield of $RO^-{}^*$ by two consecutive processes, indirect excitation of ROH* and ESDP

$$\Phi' = k_f'[RO^-{}^*]/I_a \qquad (A3)$$

and substituting eq A1, one obtains

$$\Phi' = k_f' k_{DP}[ROH^*]/I_a(k_f' + k_q') \qquad (A4)$$

Then, using the expression for [ROH*] given in eq A2 results in the expression

$$\Phi' = [k_f'/(k_f' + k_q')][k_{DP}/(k_f + k_q + k_{DP} + k_{ET})] \qquad (A5)$$

Taking into account the fluorescence quantum yield of $RO^-{}^*$ by its direct excitation in the absence of ESDP, $\Phi_0' = k_f'/(k_f' + k_q')$, one obtains an expression for the relative fluorescence quantum yield of $RO^-{}^*$

$$\Phi'/\Phi_0' = k_{DP}/(k_f + k_q + k_{DP} + k_{ET}) \qquad (A6)$$

Then, using the expressions for the fluorescence quantum yield of ROH*, namely, $\Phi = k_f/(k_f + k_q + k_{DP} + k_{ET})$ and $\Phi_0 = k_f/(k_f + k_q)$ in the presence and absence of ESDP, respectively, one finally obtains

$$(\Phi'/\Phi_0')/(\Phi/\Phi_0) = k_{DP}/(k_f + k_q) = k_{DP}\tau_0 \qquad (A7)$$

where $\tau_0 = 1/(k_f + k_q)$ is the excited-state lifetime of ROH* in the absence of ESDP.

Thereby, eq A7 is equivalent to the eq 2 in section 1.1 above.

References and Notes

(1) (a) Hall, D.; Rao, K. *Photosynthesis*; Cambridge University Press: Cambridge, U.K., 1999. (b) Baciou, H.; Michel, M. *Biochemistry* **1996**, *34*, 7967.

(2) Cui, Q.; Karplus, M. *J. Phys. Chem. B* **2002**, *106*, 7927.

(3) (a) Nicholls, D. G.; Ferguson, S. J. *Bioenergetics*; Academic Press: London, 1992. (b) Rastogi, V.; Girvin, A. *Nature* **1999**, *402*, 263.

(4) De Silva, A.; Gunaratne, H.; Gunnlaugson, Th.; Huxley, A.; McCoy, C.; Rademacher, J.; Rice, T. *Chem. Rev.* **1997**, *97*, 1515.

(5) Il'ichev, Y. V.; Solntsev, K. M.; Demyashkevich, A. B.; Kuzmin, M. G.; Lemmetyinen, K.; Vuorimaa, E. *Chem. Phys. Lett*. **1992**, *193*, 128.

(6) Zaitsev, V. B. *Surf. Sci*. **1999**, *433*, 944.

(7) (a) Weller, A. Acid base properties of electronic states. In *Progress in Reaction Kinetics*; Porter, E., Stevens, B., Eds.; Pergamon Press: Oxford, U.K., 1961; Vol. 1. (b) Shizuka, H. *Acc. Chem. Res.* **1985**, *18*, 141. (c) Tolbert, L. M.; Solntsev, K. M. *Acc. Chem. Res*. **2002**, *35*, 19. (d) Hynes, J.; Tran-Thi, T.-H.; Granucci, G. *J. Photochem. Photobiol. A* **2002**, *154*, 3.

(8) (a) Solntsev, K. M.; Huppert, D.; Agmon, N.; Tolbert, L. M. *J. Phys. Chem. A* **2000**, *104*, 4658. (b) Knochenmuss, R.; Solntsev, K. M.; Tolbert, L. M. *J. Phys. Chem. A* **2001**, *105*, 6393. (c) Knochenmuss, R.; Fischer, I. *Int. J. Mass Spectrom*. **2002**, *220*, 343. (d) Htun, M.; Suwaiyan, A.; Klein, U. *Chem. Phys. Lett*. **1995**, *243*, 71.

(9) Brown, E.; Wu, E.; Zipfel, W.; Webb, W. *Biophys. J*. **1999**, *77*, 2837.

(10) Pines, E.; Magnes, B.; Barak, T. *J. Phys. Chem. A* **2001**, *105*, 9674.

(11) (a) Laguitton-Pasquier, H.; Pevenage, D.; Ballet, P.; Vuorimaa, E.; Lemmetyinen, H.; Jeuris, K.; De Schryver, F.; Van der Auwerer, M. Space- and Time-Resolved Spectroscopy of Two-Dimensional Molecular Assemblies. In *New Trends in Fluorescence Spectroscopy*; Valeur, B., Brochon, J., Eds.; Springer: Berlin, 2001; pp 100−124. (b) Ray, K.; Nakahara, H. *J. Phys. Chem. B* **2002**, *106*, 92. (c) Kajiwara, T.; Chambers, R.; Kaerns, D. *Chem. Phys. Lett*. **1973**, *22*, 38. (d) Gabrielli, G.; Caminati, G.; Puggelli, M. *Adv. Colloid Interface Sci*. **2000**, *87*, 75. (e) Swager, T. M. *Acc. Chem. Res*. **1998**, *31*, 77.

(12) (a) Kasha, M.; Rawls, H.; El-Bayoumi, A. *Pure Appl. Chem*. **1965**, *11*, 371. (b) Kemnitz, K.; Tamai, N.; Yamazaki, I.; Nakashima, N.; Yoshihara, K. *J. Phys. Chem*. **1986**, *90*, 5094.

(13) Jankowski, A.; Stefanowicz, P.; Dobryszycki, P. *J. Photochem. Photobiol. A* **1992**, *69*, 57.

(14) Lakowicz, J. *Principles of Fluorescence Spectroscopy*; Plenum Press: New York, 1983.

(15) Kawski, A. *Fotoluminesccencja roztworów*; PWN: Warszawa, 1992 (Polish edition).

(16) Mirończyk, A.; Jankowski, A. *J. Photochem. Photobiol. A* **2002**, *153*, 89.

(17) Siano, A.; Metzler, A. *J. Chem. Phys*. **1969**, *51*, 1856.

(18) Jankowski, A. *Spectrofluorimetric Investigations of the Mechanism of Proton Transfer in Biopolymers*; Wrocław University Press: Wrocław, Poland, 1996 (in Polish, with a summary in English).

(19) Nagle, J.; Tristram-Nagle, S. *J. Membr. Biol*. **1978**, *75*, 298.

(20) Agmon, N. *J. Mol. Liquids* **2000**, *85*, 87.

(21) Sokalski, W. A.; Romanowski, H.; Jaworski, A. *Adv. Mol. Relax. Interact. Processes* **1977**, *11*, 29.

(22) Ushiyama, H.; Takatsuka, K. *J. Chem. Phys*. **2001**, *115*, 5903.